High-resolution photoemission on Ag/Au(111): Spin-orbit splitting and electronic localization of the surface state

D. Popović,[1,2] F. Reinert,[3,*] S. Hüfner,[1] V. G. Grigoryan,[4] M. Springborg,[4] H. Cercellier,[5,6] Y. Fagot-Revurat,[5] B. Kierren,[5] and D. Malterre[5]

[1]*FR 7.2 Experimentalphysik, Universität des Saarlandes, 66123 Saarbrücken, Germany*

[2]*Department of Physics, Karlstad University, 65188 Karlstad, Sweden*

[3]*Experimentelle Physik II, Universität Würzburg, 97074 Würzburg, Germany*

[4]*Physikalische Chemie, Universität des Saarlandes, 66123 Saarbrücken, Germany*

[5]*Laboratoire de Physique des Matériaux, Université Henri Poincaré, Nancy I, Boîte Postale 239, 54506 Vandœuvre-lés-Nancy, France*

[6]*Institut de Physique, Université de Neuchâtel, CH-2000 Neuchâtel, Switzerland*

(Received 21 March 2005; published 11 July 2005)

We present a detailed photoemission study of the surface state dispersion in 0–10 ML thin Ag films on Au(111). The dispersion of the *L*-gap Shockley-type surface state changes monotonically from the one of Au towards the one of Ag with increasing layer thickness indicating an extension of the wave function into the solid. High resolution photoemission (PES) enables an insight into decreasing spin-orbit splitting of the surface state in Ag-covered-Au(111). The photoemission data have been well reproduced by *ab initio* band structure calculations using the WIEN2K code. The dependence of the binding energy on the increasing silver film thickness is indicative of the localization of the surface state at the surface by comparing it with the calculated electron density of the surface state. Measurements on 10 ML Ag/Au(111) reveal the *d*-band states of Ag, but one still observes *sp*-related quantum well states of silver within the projected *sp*-band gap of gold.

DOI: 10.1103/PhysRevB.72.045419 PACS number(s): 73.20.At, 79.60.Dp, 31.15.Ar, 73.20.−r

Shockley-type surface states in the *L* gap of noble metal (111) surfaces provide a suitable model system for electronic states in two dimensions. Since high-resolution photoelectron spectroscopy (PES) has enabled a precise investigation of the intrinsic line width and the spin-orbit (SO) splitting of the surface state on Au(111),[1,2] it has become increasingly interesting to study in which way adsorbates influence it. The deposition of noble gases like Xe, Kr, or Ar in a monolayer regime shows a decrease in surface state binding energy and an increase in spin-orbit splitting up to 30% with respect to the value of pure Au(111).[3] Thin epitaxial films of other noble metals on Au(111) lead to different phenomena due to the existence of an own surface state at the respective (111) surface. The energetic positions of surface and bulk states determine the binding energies of the observed states in thin films in the vicinity of the Fermi level.[4,5]

Ag/Au(111) is an intermetallic system, exhibiting parallel epitaxy due to a very small lattice mismatch (0.2%, $a_{\mathrm{Au}}=4.0782$ Å, $a_{\mathrm{Ag}}=4.0853$ Å). Two peculiarities of Au(111) as a substrate are the so-called herringbone reconstruction of the topmost surface layer (visible also in PES,[6] its influence on the Ag film growth is discussed elsewhere[7]) and the spin-orbit splitting of the Shockley state.[1,2] The Shockley-state in Au(111) exists in the inverted *sp*-band gap due to the boundary conditions at the surface.[8] Quantum-well states in intermetallic systems are confined within the same projected *sp* bulk band gap.[9] Complementary to that, the projected band gap and the valence band carry information about the bulk or the substrate. The interesting question of probing deep interfaces, has been investigated in the past by observing the quantum-well states[9] or core-level shifts.[10] We show in this paper that the projected band structure of gold is still visible in the data after 10 ML of silver have been evaporated and when the *d* band of silver is already completely formed. The changes of the surface state are in accordance with the slower development of the *sp* bands with layer thickness. Whereas the *d* band develops together with the film, the surface state and the quantum well states offer information about the film thickness and the projected band gap enables a direct visualization of the substrate.

The photoemission experiments have been performed with a SCIENTA SES 200 analyzer in the angular mode in the UHV chamber with the base pressure 5×10^{-11} mbar. The energy resolution is $\Delta E=3.5$ meV, the angular resolution $\Delta\theta\approx\pm0.15°$.[11,12] The measurements have been performed with a monochromatized GAMMADATA VUV lamp at a photon energy of $h\nu=21.2$ eV (He I) at the sample temperature 20–30 K (Saarbrücken, SB) or with a nonmonochromatized UVS-300 SPECS discharge lamp at the photon energy of $h\nu=11.83$ eV (Ar I) and the sample temperature of 80 K (Nancy, N). The measuring time was approximately 15 min for one data set of the complete occupied surface state.

The surface of the Au(111) was prepared by repeated cycles of Ar^+ sputtering and subsequent annealing up to 700 °C (SB) or 350 °C (N). Ag films were evaporated at room temperature with triple-evaporator Omicron EFM 3T ($I_e=17$ mA, flux=1 μA, HV=690 V), at evaporation rate of 0.3 Å/min (SB) or by a Knudsen cell at evaporation rate of 0.5 ML/min (N) in the high 10^{-10} mbar pressure range. The coverage was determined by a quartz-microbalance and checked by STM (N).[7]

Band structure calculations have been performed using the WIEN2K package implementing the FLAPW (full-potential linearized augmented plane-wave) method within the framework of density functional theory (DFT).[14] For the exchange-correlation potential the generalized gradient ap-

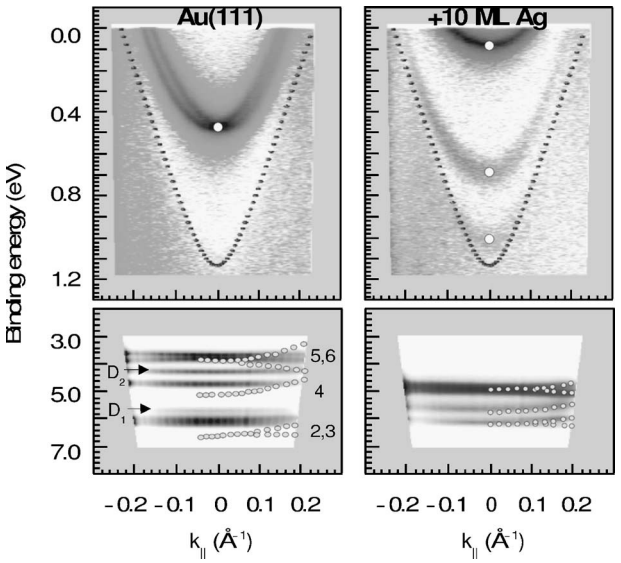

FIG. 1. Top: Surface state (lower binding energy) and quantum well states (higher binding energies) along $\bar{\Gamma}\bar{K}$ marked by white dots for Au(111) and 10 ML Ag/Au(111). Band-structure calculations of the Au *sp* gap have been shifted to fit the measured binding energy for the pure Au(111) and are shown as black circles. Bottom: valence band; 2-6 are valence bands of the Au(111), D_1 and D_2 are the surface resonances. White dots represent band-structure calculations for pure Au (left) and Ag (right) by Smith (Ref. 13). The measurements have been taken with He I at $T=20$ K.

proximation (GGA) was used.[15] A basis set of 1600 LAPWs and a 100 *k*-points mesh in the irreducible Brillouin zone have been used. SO-coupling was included in a second variational step. The surface was modeled by a periodic slab of 23 Au and correspondingly from one to six Ag layers on the each Au surface, separated by 20 bohr of vacuum. For smaller slabs, the interaction of the two confining surfaces, both via the "bulk" and via the "vacuum,"[16] leads to an artificial splitting of the surface state. For a seven-layer slab this splitting is much larger than the SO splitting of the Au(111) surface state. The size of the system, i.e., 23 layers and 20 bohr vacuum, is chosen in order to reduce the artifact below 1 meV at $k=0$, which is two orders of magnitude smaller than the SO splitting at E_F (>100 meV). The slab thickness exceeds both decay lengths of the surface state in Au(111) (3.6 ML) and Ag(111) (12 ML).[17] Finally, allowing for structural relaxation did not lead to changes observable within our experimental uncertainty.

Figure 1 shows surface and bulk valence band states for Au(111) (left) and 10 ML Ag/Au(111) (right) over a wide binding energy (BE) range, from the Fermi level down to 7 eV. The upper panels show the surface states with their band minima marked with white circles: The first two quantum well states (at 688 and 1048 meV BE for a silver covered surface) and, with higher intensity, the Shockley state (at 479 meV BE left and 84 meV BE right). The surface and quantum well states shift towards lower binding energies with increasing silver coverage within the limits of the projected bulk band gap of Au(111). The gap is visible in Fig. 1 as the light area. The black circles indicate the dispersion of the uppermost calculated bulk band, shifted by 120 meV towards E_F, to match with the experimental position. The projected band gap of Au does not change with coverage. On the other hand, the calculated "band gap minimum" is the bulk mode with the lowest binding energy. This corresponds for a couple of monolayers to the lowest quantum well state of the Ag film.

The lower panels in Fig. 1 show the energy range of the 4*d* and 5*d* bands of Ag and Au, respectively. Contributions for the Au(111) surface (left) are identified according to Refs. 18 and 19 and overlayed by the band-structure calculations from Ref. 13. The bulk bands are denoted by numbers 2–6, whereas D_1 and D_2 are surface resonances. The valence band of 10 ML Ag/Au(111) corresponds perfectly to the overlayed band-structure calculations of pure Ag taken from the Ref. 13. Both calculations for silver and gold are taken from the Ref. 13 along ΓK direction, and He I radiation should correspond to $k_\perp$ in the vicinity of Γ.[20,21] However, the measurement paths on Au and Ag are differently displaced from Γ, which leads to different agreement between the calculation and the measurement for Au and Ag. The number and the splitting of the Au-bands are observed experimentally, their BEs are somewhat overestimated. One sees by comparison with the measurements that due to the small sampling depth of PES (at He I ~5–10 Å)[22] the Au-bands are absent for 10 ML Ag/Au(111) and that the measured valence band corresponds completely to the one of bulk silver. Although the *d* bands are already the ones of bulk silver, the upper panel for the 10 ML system still shows the *L* gap of the Au(111) substrate lying ≈30 Å below the surface. The projected *sp*-band structure of Ag will evolve from the quantum-

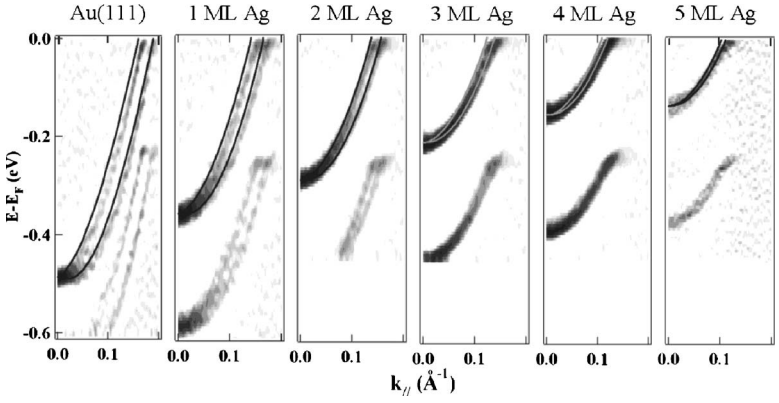

FIG. 2. Surface state dispersion changes with silver coverage taken with Ar I. The grey-scale maps represent the second derivative of the measured intensity. The calculations of the Shockley state (black lines) have been shifted for each coverage to fit the measured binding energies. The replica at higher BEs is due to the Ar satellite.

TABLE I. Binding energy (BE), effective mass, and spin-orbit splitting (SOS) of the surface state for the corresponding coverages of Ag on Au(111) as obtained from the band-structure calculations (superscript th) and as measured (superscript exp).

Surface	BE^{th}(meV)	BE^{exp}(meV)	m^*/m_e^{th}	m^*/m_e^{exp}	$SOS^{th}(\Delta k_{\|})(\text{Å}^{-1})$	$SOS^{exp}(\Delta k_{\|})(\text{Å}^{-1})$
Au(111)	429	487	0.23	0.26	0.030	0.023
+1 ML Ag	409	305	0.28	0.33	0.023	0.019
+2 ML Ag	334	222	0.32	0.34	0.019	0.015
+3 ML Ag	274	184	0.35	0.38	0.014	0.013
+4 ML Ag	235	158	0.36	0.40	0.011	0.013
+5 ML Ag	223	98	0.36	0.41	0.009	0.010
+6 ML Ag	194	77[a]	0.37		0.007	<0.010
Ag(111)	178	64	0.37	0.42	0.004	<0.010

[a]Measured at 90 K (Refs. 7 and 24).

well states and reach the position of the Ag *sp*-gap BE minimum after several tens of monolayers, according to the previously reported "slower" development of the *sp* bands of the adsorbate by comparison with the *d* bands.[23] This is related to the highly localized character of the *d* bands and, contrary to that, free-electron-like character of the extended *s* states, which are thus sensitive to the projected gap and quantum-well boundaries.

The evolution of the surface state with Ag coverage is depicted in Fig. 2. The gray-scale maps represent the second derivative of the measured intensity. The replica of the surface state, appearing at higher binding energies, is due to the Ar satellite. With increasing Ag layer thickness one can clearly observe a shift of the surface state towards the Fermi level and a decrease of the spin-orbit splitting. A fit of the dispersion by two parabolas allows a more detailed analysis and yields the values for the maximum binding energy, the effective mass and the SOS given in Table I). Obviously all three parameters show a monotonous change from the values of pure Au(111) towards the values of Ag(111).

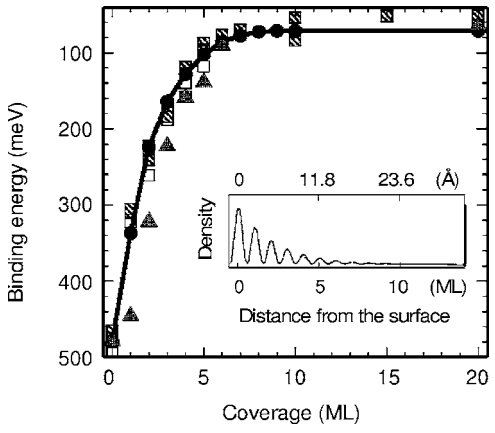

FIG. 3. Ag-coverage dependent surface state binding energy: Experimental data using He I (shaded squares) and Ar I (white squares) radiation, band-structure calculations (triangles) and electron density of the surface state (see the inset) distributed over discrete numbers of monolayers (circles and line) both scaled between the binding energies of clean Ag(111) and Au(111) as reference points. The inset shows NFE calculations of the surface-state electron density perpendicular to the surface by Beckmann (Ref. 25) for 12 ML Ag/Au(111).

The black lines in Fig. 2 represent the result of our band structure calculations. Because the exact position of the Fermi level is often a problem in DFT results, it was necessary to shift the calculated surface state dispersions in energy to the position of the experimental result (values are given in Table I). The calculated effective masses and the spin-orbit splitting are in agreement with the experimental values.

Figure 3 presents the dependence of the measured and calculated BEs on the Ag film thickness. The squares represent the results of several measurements, obtained with different film preparation techniques and using He I or Ar I radiation. Thus, one gets insight into the data spread which could originate from different surface preparations or coverage calibrations. In spite of the observed differences, the BEs of all measured surface states agree reasonably well. Beside the measurements, the *ab initio* band structure calculations of the surface state are presented (triangles), scaled linearly between the two reference points at 0 ML [clean Au(111)] and 20 ML [for which we take the parameters of the clean Ag(111) surface]. The calculated binding energies (triangles) reproduce very well the changes of the measured binding energy with the Ag coverage.

The observed changes in surface state dispersion can be explained by closer inspection of the electron density as a function of the distance from the surface. The inset in Fig. 3 displays the result of a nearly free electron approximation for the electron density of a Au(111) surface covered by 12 ML of Ag.[25] Because the decay length is of the order of the overlayer thickness, the displayed electron density represents roughly the one of pure Ag(111). The plot shows that more than 80% of the surface state electrons are localized within the first 5 MLs. The electron density distribution can be used to illustrate the dependence of the BE on the layer thickness. If we use the electron density, integrated over the Ag overlayer thickness, as a weighting factor for the binding energies of pure Au(111) and Ag(111), we get the solid line in Fig. 3. The good agreement shows, that the surface state properties of the overlayer system can be decomposed in contributions from the two components. It demonstrates the exponential development of the Ag contribution in the BE of the surface state, which is related to the silver contribution to the total

number of atoms within the decay length of the surface state. It describes the measured binding energies perfectly.

We have presented high-resolution photoemission data of the *L*-gap Shockley states for 0–10 epitaxially grown ML of silver on Au(111). The Shockley state exhibits gradual changes with the layer thickness and the values of the relevant surface state parameters, describing the band dispersion, evolve from the ones of gold into the ones of silver. High-resolution photoemission has enabled the direct observation of the decrease of the spin-orbit splitting of the surface state with silver coverage. Good agreement is achieved between *ab initio* band structure slab-layer calculations embedded in the WIEN2K code and the photoemission data: The surface state band parameters are well reproduced by the theory, except for the value of the Fermi level, which is too high in the calculations. However, the relative shifts depending on the overlayer thickness are described by the calculations and can intuitively be explained by the distribution of the electron density decaying into the crystal volume. Whereas the localized *d*-bands are already bulk-like for 10 ML, the *sp* gap of the system is still the one of the substrate, thus influencing the surface state which forms within the gap, even if the coverage thickness exceeds the photoelectron mean free path significantly. On the other hand, the good agreement of the slab-layer calculations with the experiment shows that this method is able to reproduce details of the surface electronic structure and can therefore be used to investigate interface systems theoretically. Furthermore, the characteristic changes of the surface state due to modifications of the surface and thus induced different changes of the *d* or *sp* bands, together with the possibility of a numerical reproduction by *ab initio* methods make the surface related states capable of providing important information about surface processes and interfaces.

ACKNOWLEDGMENTS

This work was financially supported by the Deutsche Forschungsgemeinschaft (SFB 277). M.S. and V.G.G. gratefully acknowledge Fonds der Chemischen Industrie for very generous support.

*Electronic address: reinert@physik.uni-wuerzburg.de

[1] F. Reinert, J. Phys.: Condens. Matter **15**, S693 (2003).
[2] G. Nicolay, F. Reinert, S. Hüfner, and P. Blaha, Phys. Rev. B **65**, 033407 (2001).
[3] F. Forster, G. Nicolay, F. Reinert, D. Ehm, S. Schmidt, and S. Hüfner, Surf. Sci. **532-535**, 160 (2003).
[4] A. Bendounan, Y. Fagot-Revurat, B. Kierren, F. Bertran, V. Yu. Yurov, and D. Malterre, Surf. Sci. **496**, L43 (2002).
[5] A. Bendounan, H. Cercellier, Y. Fagot-Revurat, B. Kierren, V. Yu. Yurov, and D. Malterre, Phys. Rev. B **67**, 165412 (2003).
[6] F. Reinert and G. Nicolay, Appl. Phys. A: Mater. Sci. Process. **78**, 817 (2004).
[7] H. Cercellier, Y. Fagot-Revurat, B. Kierren, D. Malterre, and F. Reinert, Surf. Sci. **566**, 520 (2004).
[8] W. Shockley, Phys. Rev. **56**, 317 (1939).
[9] T. Miller, A. Samsavar, G. Franklin, and T.-C. Chiang, Phys. Rev. Lett. **61**, 1404 (1988).
[10] T. Hsieh, T. Miller, and T.-C. Chiang, Phys. Rev. B **33**, 2865 (1986).
[11] F. Reinert, G. Nicolay, S. Schmidt, D. Ehm, and S. Hüfner, Phys. Rev. B **63**, 115415 (2001).
[12] G. Nicolay, F. Reinert, S. Schmidt, D. Ehm, P. Steiner, and S. Hüfner, Phys. Rev. B **62**, 1631 (2000).
[13] N. Smith, Phys. Rev. B **9**, 1365 (1974).
[14] P. Blaha, K. Schwarz, G. K. H. Madsen, D. Kvasnicka, and J. Luitz, WIEN2K, *An Augmented Plane Wave+Local Orbitals Program for Calculating Crystal Properties* (Karlheinz Schwarz, Techn. Universität Wien, Austria, 2001), ISBN 3-9501031-1-2.
[15] J. P. Perdew, K. Burke, and M. Ernzerhof, Phys. Rev. Lett. **77**, 3865 (1996).
[16] N. Takeuchi, C. T. Chan, and K. M. Ho, Phys. Rev. B **43**, 13899 (1991).
[17] T. C. Hsieh and T. Chiang, Surf. Sci. **166**, 554 (1986).
[18] J. Nelson, S. Kim, W. Gignac, R. Williams, J. Tobin, S. Robey, and D. Shirley, Phys. Rev. B **32**, 3465 (1985).
[19] R. Paniago, R. Matzdorf, and A. Goldmann, Europhys. Lett. **26**, 63 (1994).
[20] P. Wehner, R. Williams, S. Kevan, D. Denley, and D. Shirley, Phys. Rev. B **19**, 6164 (1979).
[21] K. Mills, R. Davis, S. Kevan, G. Thornton, and D. Shirley, Phys. Rev. B **22**, 581 (1980).
[22] S. Hüfner, *Photoelectron spectroscopy* (Springer-Verlag, Germany, 2003), 3rd ed.
[23] J. G. Tobin, S. W. Robey, L. E. Klebanoff, and D. A. Shirley, Phys. Rev. B **35**, 9056 (1987).
[24] H. Cercellier, Y. Fagot-Revurat, B. Kierren, F. Reinert, D. Popović, and D. Malterre, Phys. Rev. B **70**, 193412 (2004).
[25] A. Beckmann, M. Klaua, and K. Meinel, Phys. Rev. B **48**, 1844 (1993).